

See discussions, stats, and author profiles for this publication at: <https://www.researchgate.net/publication/231644561>

Nano/Microstructure Fabrication of Functional Organic Material: Polymorphic Structure and Tunable Luminescence

ARTICLE *in* THE JOURNAL OF PHYSICAL CHEMISTRY C · JUNE 2010

Impact Factor: 4.77 · DOI: 10.1021/jp100594w

CITATIONS

32

READS

38

2 AUTHORS, INCLUDING:



Savarimuthu Philip Anthony

SASTRA University

64 PUBLICATIONS 566 CITATIONS

[SEE PROFILE](#)

Nano/Microstructure Fabrication of Functional Organic Material: Polymorphic Structure and Tunable Luminescence

Savarimuthu Philip Anthony and Sylvia M. Draper*

School of Chemistry, Trinity College Dublin, Dublin-2, Ireland

Received: January 21, 2010; Revised Manuscript Received: May 28, 2010

Nano/microstructure fabrication of 2-cyano-3(4-(diphenylamino)phenyl) acrylic acid (CDPA), an organic optoelectronic material, via a simple reprecipitation method produces particles with a different morphology, phase, and structure and a tailored luminescence. Spherical amorphous, diamond, and multifaceted microcrystals of CDPA were obtained by optimizing the fabrication conditions. CDPA with rod-like morphology was produced on the introduction of polymer additives to the growth solution. A polymorph of CDPA, not observed in the usual solution crystallization process, was obtained as 1D nanowires (200–400 nm (width) and 3–20 μm (length)). Powder X-ray diffraction and optical studies demonstrate the polymorphic structure of the nanowires. Scanning electron and confocal fluorescence microscopy, respectively, were used to demonstrate the different morphologies of fabricated nano/microstructures and the luminescence tuning (from 604 to 519 nm).

Introduction

Functional organic materials composed of optically and electronically active constituents have received recent interest in nanoscience and nanotechnology.^{1–11} The tunable physical properties of organic nanomaterials in terms of their size,^{1–3} shape,^{4–7} and crystallinity^{8,11} are expected to provide an opportunity to control optoelectronic properties and therefore device performance. For example, one-dimensional (1D) single crystalline nanostructures, such as nanowires, nanorods, and nanoribbons, have been shown to be potential candidates for the construction of optical waveguides, lasers, and field effect transistors.^{12–14} In addition, the luminescent properties of organic materials, emerging as a result of the special aggregation modes of the organic molecules and the crystallinity of the materials, have been successfully tuned through nanofabrication.^{12,13,15–18} Indeed, nanowires of organic luminescent materials have displayed enhanced sensor properties.^{19,20}

Despite the myriad of advantages, the fabrication of organic nanomaterials with defined size, morphology, and function remains a considerable challenge. The problem is the multitude of cooperative and simultaneous intermolecular interactions (hydrogen bonding, van der Waals, π – π stacking, and electrostatics) that arise to produce the final structure.^{21–23} Extended π -conjugated systems that self-assemble through π – π stacking are commonly employed for the fabrication of 1D organic nanostructures.^{12–14,24,25} The direction of dipole–dipole interactions between molecules have been proposed by Zhang et al. to control the preferential growth of nanostructures.^{26,27} In donor–acceptor molecules, hydrogen bond functionality plays a key role in the formation of 1D nanowires or platelets.²⁸ The size and shape of the nano/microcrystals can be affected by many factors, principally the concentration^{29–31} and temperature.^{1,2,30,31} Additives, such as surfactants, and macromolecules, which mainly act as crystal growth inhibitors, can also be used to alter or control the nanostructure morphology and crystal size.^{29,30,32}

Although it is unpredictable, polymorphism, the ability of a material to adopt more than one form, offers an attractive approach to tune and switch the solid state luminescent properties without the need for multistep synthesis because the optical properties of materials are controlled by molecular organization.^{33–35} The generation of polymorphic structure mostly relies on the manipulations of conditions such as solvent, temperature, and mode of crystallization.³⁶ Nanofabrications have been successfully used to control the size, shape, and crystallinity of functional organic materials, but formation of polymorphic structure by nanofabrication is less studied,^{37,38} except in the nanostructures of macromolecules and organogels.^{39,40}

Triphenylamine derivatives have enjoyed widespread use as hole transporting materials, emitting layers in electroluminescent diodes, light harvesters in dye-sensitized solar cells, and nonlinear optical materials.^{41–43} Interestingly, triphenylamine derivatives with their propellerlike shape often exhibit solid state luminescent properties.⁴⁴ Octupolar tris(4-cyanophenyl)amine-based nano/microcrystals exhibit strong luminescence and optical limiting properties.⁴⁵ CDPA, 2-cyano-3(4-(diphenylamino)phenyl)acrylic acid, a triphenylamine-based dye, is an important organic material that exhibits intense luminescence in solution as well as in the solid state and moderate efficiency in dye-sensitized solar cells.^{43,46} The carboxylic acid of CDPA displays interesting supramolecular interactions when mixed with amines and in several cases leads to the formation of luminescent host systems with included solvent molecules. Recently, we reported the supramolecular luminescent systems based on CDPA and amines that exhibit unusual intermolecular interactions with tunable and switchable solid state luminescence.⁴⁶ Herein, we report the nano/microstructure fabrication of CDPA using a simple reprecipitation method. CDPA forms as spherical amorphous, diamond-shaped, multifaceted microcrystals and 1D nanowires depending on the concentrations of CDPA and the solution to be introduced (HCl). The presence of polymer additives in the growth solution leads to the formation of 1D rods. Optical and powder X-ray diffraction studies revealed that the 1D nanowire is a polymorph of CDPA.

* To whom the correspondence should be addressed. Phone: +35318962026, Fax: +35316712826, E-mail: smdraper@tcd.ie.

More importantly, changes in phase, morphology, and structure are accompanied by changes in the observed luminescence.

Experimental Section

Chemicals. Anhydrous acetonitrile (CH_3CN , HPLC grade), poly(sodium 4-styrenesulphonate) (PSS, MW = 70000), poly(acrylic acid) sodium salt (PAA, MW = 5100 g mol⁻¹), and HCl (98%) were purchased commercially and used without further purification. Ultrapure water, produced using a Milli-Q apparatus (Millipore), was used in all experiments.

Synthesis of CDPA. A 70 mL acetonitrile solution of 4-diphenylaminobenzaldehyde (1.0 g, 3.66 mmol), cyanoacetic acid (0.34 g, 4.0 mmol), and piperidine (0.62 g, 7.32 mmol) was refluxed for 4 h under a nitrogen atmosphere. Solvent removal by rotary evaporator followed by solvent extraction (CH_2Cl_2 and aq HCl (0.1 M)) yielded the product as a dark purple solid (1.05 g, 85%): mp 213–214 °C. ¹H NMR (500 MHz, CDCl_3) δ 8.15 (s, 1H), 7.90 (d, 2H), 7.39 (t, 4H), 7.23 (m, 6H), 6.98 (d, 2H). ¹³C NMR (125 MHz, CDCl_3) δ 168.5, 155.0, 153.2, 145.1, 132.7, 129.6, 126.3, 125.5, 122.8, 118.2, 116.9, 95.5.

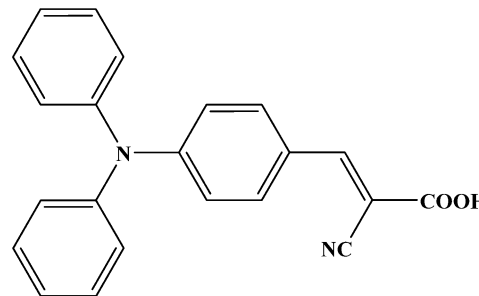
Synthesis of CDPA Colloidal Particles. Typically, a 10 mL stock solution of CDPA in CH_3CN with different concentrations (10^{-4} , 10^{-3} , and 5×10^{-3} M) were prepared. Different volumes of the stock solution (0.1, 0.3, 0.5, 0.6, 0.8, 1 mL) were rapidly introduced into 25 mL of 0.2 M HCl or 25 mL of 0.2 M HCl containing PAA or PSS (1 wt %) polymer additives (0.25 g of polymer in 24.75 g of water) or 25 mL of 0.02 M HCl solution under sonication. Sonoication was continued for an additional 20 min. The samples were left undisturbed for 1 week before microscopy evaluation. The nano/microstructures of CDPA were collected on the surface of an alumina membrane with a pore size of 0.02 μm (Whatman International, Ltd.) and dried under vacuum for microscopy analysis. Spectroscopic analysis of the nanoparticles was carried out while keeping the sample directly in the solution. The morphology and size of the micro/nanoparticles formed were confirmed as stable for more than 2 months.

Microscopy Characterization. The morphologies and sizes of the samples were examined using field emission scanning electron microscopy (FE-SEM, Hitachi S-4300) at an acceleration voltage of 5 kV. Prior to analysis, the samples were coated with a thin layer of gold. The confocal microscopy images of the nanostructures were obtained from an Olympus FV1000 laser scanning Confocal Microscope, using a UPlanFLN 40x/1.30 NA oil objective. The samples were prepared by placing a drop of colloidal solution onto a clean glass slide.

Structural Analysis. The powder X-ray diffraction (PXRD) patterns were measured using a Siemens D500 X-ray diffractometer with Cu K α radiation ($\lambda = 1.54050 \text{ \AA}$) operated in the 2θ range from 10° to 40° .

Spectroscopy Characterization. Absorption and luminescence spectra were recorded using a Perkin-Elmer Lambda 1050 and Horiba Jobin Yvon Fluorolog instrument. Fluorescence lifetime and luminescence spectra of nano/microstructures and solid samples were measured by keeping them in a quartz cell and NMR tube, respectively. The NMR tube was placed in the beam path using a set up provided by the Horiba Jobin Yvon Fluorolog recording the low temperature emission spectrum for solid samples. The optical density of the colloid samples was maintained at a low level (≤ 0.1) by diluting with the required amount of HCl–water to avoid any inner-filter effect. Fluorescence decay profiles of the samples were recorded using a single photon counting spectrophotofluorimeter. The sample was excited by

SCHEME 1: Molecular Structure of CDPA



using nanodiodes (370 nm) and the decays were monitored at the corresponding emission maximum of the compounds. Data scan software was used for fitting the decay spectra ($\chi^2 = 1$ –1.3) and yielded the fluorescence lifetimes. NMR spectra were obtained using a Bruker 400 MHz instrument. Diffused reflectance Infrared (IR) spectra were performed on a Perkin-Elmer spectrum 100, FT-IR spectrometer instrument. Nanowires were filtered, washed with distilled water, and dried before using for NMR and IR studies.

Results and Discussion

Organic dye, CDPA (Scheme 1), a triphenylamine derivative, was synthesized following the literature procedure.⁴⁷ CDPA exhibits strong luminescence in CH_2Cl_2 solutions with λ_{max} at 603 nm and an estimated quantum yield (Φ_F) of 0.165 (in comparison with coumarin 6). Solid CDPA has a similar luminescence intensity. Different CH_3CN solution of CDPA were prepared (10^{-4} , 10^{-3} , and 5×10^{-3} M) from which small volumes were taken and rapidly injected into 25 mL of 0.2 or 0.02 M HCl solution under sonoication to generate samples **1**–**11** (see Table 1). Nano/microparticles were not formed from the injection of CDPA– CH_3CN solutions into water (irrespective of concentration or prolonged standing (>1 week)) due to the slight solubility of CDPA in water. Only an injection into acidic aqueous solutions, in which CDPA is not soluble, produces nano/microparticles (within 1–2 days).

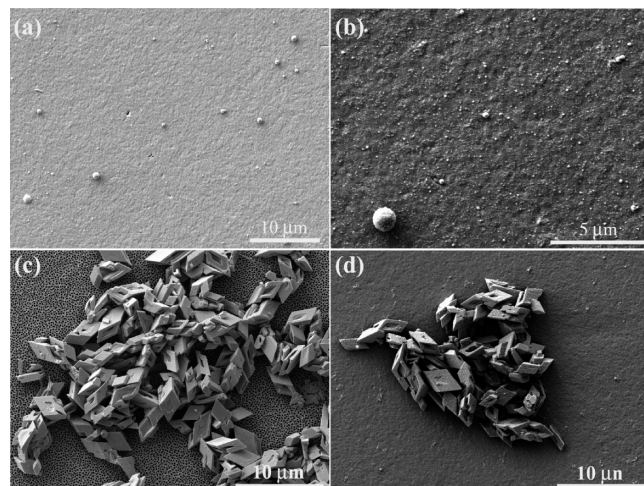
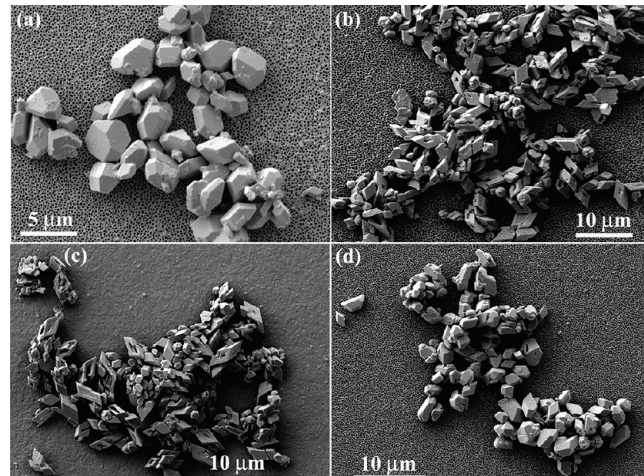
The morphology of the nano/microparticles formed by each sample (**1**–**11**) was investigated by FE-SEM. **1** and **2** form stable, spherical amorphous nano/microparticles (Figure 1a, b), with broad size distribution (50 nm to 1 μm). These remain unchanged after standing for prolonged periods (3 months). Increasing the concentration or amount of CDPA– CH_3CN solution, as in **3** and **4**, produces diamond-shaped microcrystals (approximately 2–4 μm , Figure 1c,d). In samples **1** and **2**, possibly as a result of the low CDPA concentrations, growth stops at spherical amorphous particles. Further increases in the injecting volume of CDPA– CH_3CN from 5×10^{-3} concentration (**5** and **6**) produces diamond-shaped microcrystals along with multifaceted microcrystals between 2–3 μm in size (Figure 2a,b). In the case of **5**, 92% of multifaceted microcrystals and 8% diamond-shaped crystals were formed and in **6**, multifaceted microcrystals accounted for 29% and diamond-shaped microcrystals forms 71%.

The strong influence of additives such as dendrimers, DNA, and linear polymers on the growth kinetics and microcrystalline morphology of the organic dye, 7-nitrobenz-2-oxa-1,3-diazol-4-yl, have been reported.^{48–50} Recently, Lei et al. utilized amphiphilic ligands to control the morphology of perylene, giving square and rhombus sheet structures.⁵¹ These effects were attributed to the preferential adsorption or interaction of additives on particular surfaces of the microcrystal such that interference occurs in the crystal growth along that direction.

TABLE 1: Nano/Microstructure Fabrication of CDPA in Different Conditions

sample	concen of CDPA in CH_3CN (M)	volume of CDPA used (mL)	concen of HCl (M)	polymer additives	nano/microstructure morphology
1	10^{-4}	0.5	0.2	PAA PSS	spherical amorphous
2	10^{-3}	0.1	0.2		spherical amorphous
3	10^{-3}	0.5	0.2		diamond-shaped microcrystals
4	5×10^{-3}	0.1	0.2		diamond-shaped microcrystals
5	5×10^{-3}	0.3	0.2		multifaceted/diamond-shaped microcrystals
6	5×10^{-3}	0.6	0.2		multifaceted/diamond-shaped microcrystals
7	10^{-3}	0.5	0.2		1D rods
8	10^{-3}	0.5	0.2		1D rods
9	10^{-3}	0.5	0.02		1D nanowires
10	5×10^{-3}	0.5	0.02		1D nanowires/rods/diamond-shaped microcrystals
11	10^{-2}	0.5	0.02		rods/diamond-shaped microcrystals

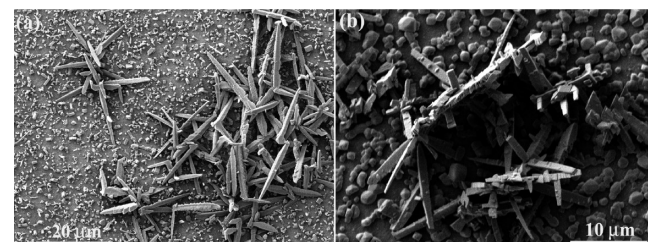
In this study, PAA (poly(acrylic acid) sodium salt) and PSS (poly(sodium 4-styrenesulphonate) were used to investigate the consequence of polymer additives to the growth morphology of CDPA, which possesses both hydrophilic carboxylic acid and hydrophobic aromatic groups. The presence of PAA (**7**) and PSS (**8**) additives led to the formation of 1D rods and no diamond-shaped microcrystals (Figure 3; width 1 μm , length 15 μm (**7**) and width 1 μm , length 10 μm (**8**)). This result occurred irrespective of the concentration of CDPA– CH_3CN ; for example, even 10⁻⁴ M concentrations of CDPA– CH_3CN

**Figure 1.** FE-SEM images of sample 1–4 (refer to Table 1).**Figure 2.** FE-SEM images of samples 5 (a) and 6 (b) (refer to Table 1). (c and d) The morphology of CDPA microcrystals obtained by injecting a higher volume (0.8 and 1 mL) than used for 5 and 6 from 5×10^{-3} M concentration into 0.2 M HCl.

solutions, which produced spherical amorphous particles, gave crystalline 1D rodlike morphology in the presence of additives.

Single-crystal X-ray analysis of CDPA reveals strong H-bonding interactions between the carboxylic acid and cyano groups together with other weak interactions (Figure S1 in the Supporting Information).⁴⁵ The diamond-shaped and multifaceted microcrystals were expected to grow through similar intermolecular interactions. The presence of PAA and PSS additives, with hydrophilic carboxylic and sulfonic acid groups, might interfere with this crystal growth by forming intermolecular H-bond interactions with the carboxylic acid or cyano groups of CDPA. This interference might have forced the CDPA molecules to assemble through other interactions such as C–H \cdots π into 1D rods. The 1D rods generated in the presence of PAA or PSS grow from a common axis; further multiple growth sites were observed only in the rods obtained in PSS (**8**). In addition to rods, several particles with different morphology such as cubes were also observed in FE-SEM of **7** and **8**, but these are sodium chloride or polymer particles (confocal fluorescence microscopy is discussed later).

Interestingly, a dilution of poor solvent concentration (HCl from 0.2 to 0.02 M) leads to the formation of 1D nanowires of CDPA. Highly reproducible CDPA nanowires (200–400 nm width and up to 20 μm long) were obtained by injecting 0.5 mL of 10⁻³ M (**9**) solution into 0.02 M HCl (Figure 4a). Nanowires were stable in solution for more than three months. Increasing the concentration of the injected CDPA solution, for example, injecting 0.5 mL of a 5×10^{-3} M into 0.02 M HCl (**10**) led to the formation of diamond-shaped microcrystals (45%), nanowires (54%), and rods (1%; Figure 4b). Further increasing the concentration of CDPA solution to 10⁻² M (**11**) produced diamond-shaped microcrystals (96%) and micrometer-sized rods (4%) of CDPA but no nanowires (Figure 4c). The formation of 1D rods without the polymer additives indicates that CDPA can form in two different morphologies and that both rods and microcrystals are forming together. Polymer additives appear to be important to the formation of 1D rods alone. They might be playing the role of a template, bringing

**Figure 3.** FE-SEM images of sample 7 (a) and 8 (b) (refer to Table 1).

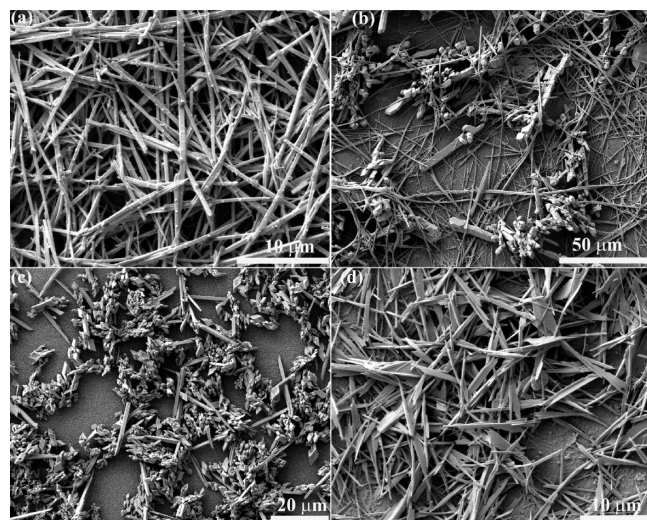


Figure 4. FE-SEM images of samples **9–11** (a, b, c; refer to Table 1), and d shows the morphology of CDPA 1D nanostructure obtained by injecting 0.3 mL (10^{-3} M) into 0.02 M HCl containing PAA polymer additives.

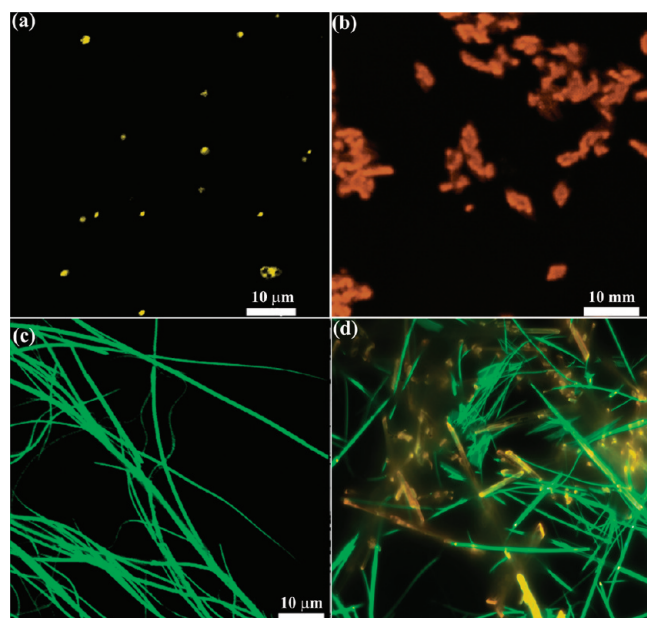


Figure 5. Confocal fluorescence microscopy images of **1**, **3**, **9**, and **10** (refer to Table 1).

together the smaller microcrystals, or they might be suppressing the growth of microcrystals to promote the growth of 1D rods. In an additional experiment, the injection of 0.5 mL of 10^{-3} M CDPA–CH₃CN solution to the growth solution (0.02 M HCl) containing PAA additives (**12**) lead to the formation of 1D thin plates (Figure 4d).

The intense solid state luminescence property of CDPA meant that confocal fluorescence microscopy was a useful tool to investigate the morphology of the nano/microstructures formed as a function of luminescence (Figure 5). The morphological changes of samples **1–8** were clearly observed using fluorescence microscopy in addition to the phase and morphology dependent luminescence. Samples **1** and **2** present clear spherical particles with yellow luminescence ($\lambda_{\text{max}} = 551$ nm), and **3–6** exhibit microcrystals with an orange luminescence ($\lambda_{\text{max}} = 587–604$ nm; Figure 5a, b). Fluorescence microscopy confirms that the rods grown in the presence of PAA or PSS additives are CDPA, as these show orange luminescence ($\lambda_{\text{max}} = 604$

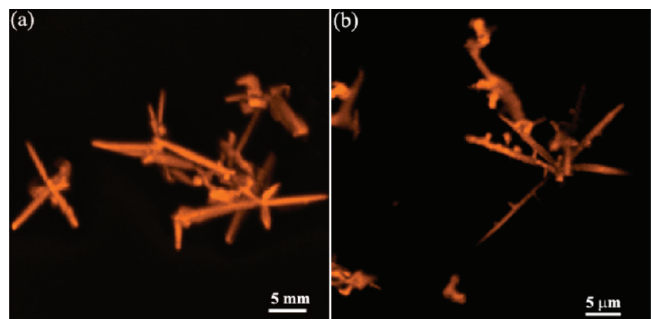


Figure 6. Confocal fluorescence microscopy images of **7** (a) and **8** (b; refer to Table 1).

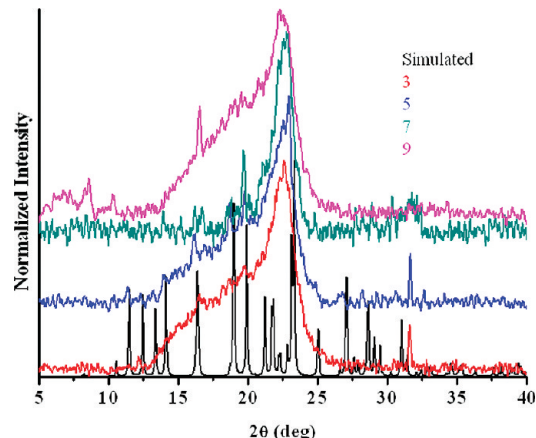


Figure 7. PXRD patterns of **3**, **5**, **7**, and **9** (refer to Table 1).

nm; Figure 6). It also shows that the other morphologies, such as cubes, which were observed in FE-SEM, belong to either sodium chloride or polymer particles, as these are nonfluorescent. The optical images of the same area clearly show the presence of other particles with different morphology (Figure S2 in the Supporting Information). Fluorescent microscopy confirms the growth arrangement of multiple rods around a common axis and that the multiple growths observed in a single rod obtained from PSS are indeed CDPA. The nanowires from **9** show blue-green luminescence from the entire nanowire (Figure 5c). The formation of nanowires and microrods, along with microcrystals, in **10** is also evident from the confocal fluorescence images (Figure 5d) and exhibit blue-green luminescence for nanowires and orange luminescence for rods and microcrystals.

PXRD analysis was used to explore whether the morphology differences observed in nano/microstructures are arising from the differences in crystal habit or from the formation of different polymorphs. As expected, **1** and **2** did not show any diffraction peaks, confirming the amorphous character of the spherical particles. The microcrystals and 1D rods of **3–8** show sharp peaks in PXRD, and the patterns were compared with the simulated PXRD pattern obtained from CDPA single crystal data (Figure 7). The recorded PXRD patterns essentially match that of simulated, ruling out the possibility of polymorphism. Thus, the PXRD patterns of microcrystals (diamond and multifaceted) and 1D rods (formed with and without polymer additives) closely resemble the single-crystal CDPA PXRD pattern.

However, the PXRD of the nanowires (**9**) are different to the single-crystal CDPA PXRD pattern (Figure 7) indicating that these are a polymorph of CDPA. The PXRD of **9** exhibits broad and sharp PXRD peaks (2θ at 6.74, 8.6, 10.31, 16.55,

SCHEME 2: Dimerized Structure of CDPA through H-Bond (red) Interactions of Carboxylic Acid and Cyano Group

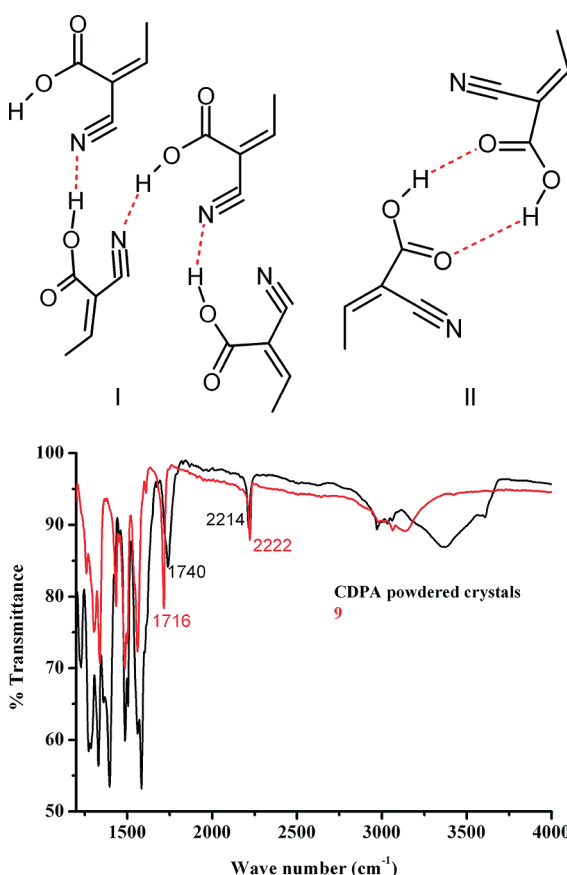


Figure 8. IR spectra of CDPA powdered crystals and **9**.

and 22.28°). The polymorphic structure of **9** was further confirmed by IR spectroscopic. The solution NMR of the nanowires is unchanged from that of bulk CDPA. It is important to note that CDPA crystals grown from various solvents (DCM, CHCl₃, EtOAc, MeOH, EtOH, toluene, CH₃CN) did not show any polymorphism.

The driving force for the formation of polymorphic nanowires is not clear and probably a complex balance of several factors. One possibility is that the repulsive forces between acidic water and the phenyl groups of CDPA might be directing the molecules to aggregate via C—H- π interactions, or at certain concentrations acid...acid intermolecular interactions dominate over intermolecular carboxylic acid/cyano interactions (Scheme 2). The IR spectra of the nanowires show C≡N and C=O absorptions at 2222 and 1716 cm⁻¹, respectively (Figure 8). The former is not shifted significantly from that of aromatic or conjugated C≡N (2222 cm⁻¹), suggesting that the cyano group in the nanowires is not involved in any or strong H-bond interactions. The shift to lower frequency of the C=O absorption (C=O in free carboxylic acid absorbs at 1760 cm⁻¹ and in H-bonded dimers between 1720–1706 cm⁻¹) and the broad absorption around 3300 cm⁻¹ indicates the possible formation of acid...acid (type-II) dimer type intermolecular H-bond interactions.⁵² In contrast, the strongly H-bonded cyano and free C=O carboxylic acid groups of bulk CDPA (type-I) absorb at 2214 and 1740 cm⁻¹, respectively.

Figure 9a,b shows the time-dependent absorption and luminescence spectra of **1**. Dilute CH₃CN solutions of CDPA exhibit absorption maxima (λ_{max}) at 419 nm; however, on

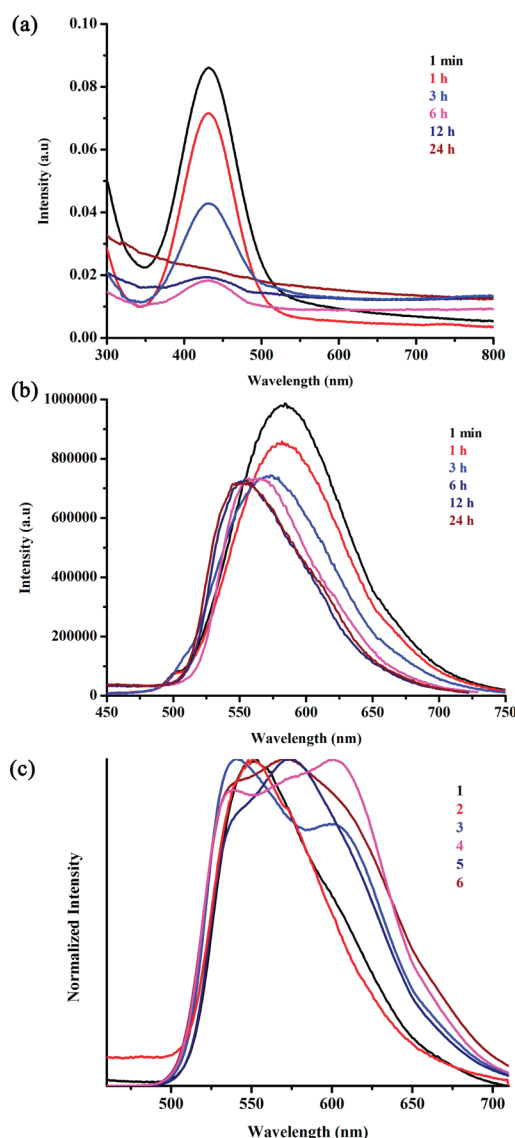


Figure 9. Time-dependent absorption (a), luminescence (b) spectra of **1** and luminescence spectra of **1–6** (refer to Table 1).

injection into acidic water, this intense intramolecular charge transfer absorption red shifts λ_{max} to 430 nm, consistent with the increased polarity of the media. The intensity of the absorption peak gradually decreases with time without change in λ_{max} , although the spectrum becomes broadened. After 24 h, the absorption at 430 nm disappears and only a broad flat line appears in the absorption spectrum. However, time-dependent excitation spectra (Figure S4) clearly exhibit two new broad signals at 366 and 500 nm. Solid CDPA (powdered materials) also exhibit a similar excitation spectrum. In general, the optical properties of dyes are modified upon aggregation or crystallization in the solid state as a consequence of interactions between transition dipole moments on different molecules. For π -conjugated molecules, the principal transition dipole moment is oriented along the molecular axis, with another dipole along the short molecular axis.⁵³ When two adjacent molecules are oriented along the same axis, the excited state will split into two exciton levels by a Davydov interaction. The magnitude of the Davydov splitting depends on the intermolecular distance. According to exciton theory, the number of exciton bands corresponds to the number of translationally inequivalent molecules per unit cell.⁵⁴ CDPA

TABLE 2: Fluorescence Lifetimes (τ_f)^a

sample	τ_1 (ns)	τ_2 (ns)	χ^2
CDPA-CH ₃ CN (511 nm)	1.733874		1.004136
CDPA crystals (604 nm)	9.56807	2.972946	1.038992
powdered CDPA (587 nm)	2.562199 (81.12%)	5.420602 (18.88%)	1.023432
1 (551 nm)	1.171105 (33.82%)	2.544279 (66.18%)	1.046954
3 541 nm	1.770186 (45.28%)	3.363147 (54.72%)	1.014061
3 604 nm	2.853605 (72.88%)	6.553329 (27.12%)	1.107362
5 (587 nm)	2.153604 (54.45%)	5.168877 (45.55%)	1.006377
7 (604 nm)	2.577657 (77.49%)	6.129538 (22.51%)	1.167448
9 (519 nm)	1.981481		1.053376

^a Decay monitored at corresponding emission maxima and $\lambda_{\text{exc}} = 370$ nm.

shows two translationally inequivalent molecules in the unit cell (Figure S4 in the Supporting Information) and hence exhibits two exciton bands in the excitation spectrum. Similar to the published work,⁵⁵ the two transitions are perpendicularly polarized. This can be understood by considering the transition dipole moments of the individual molecules in the 2-D organic plane (Figure S4 in the Supporting Information). Two dipole arrangements are predicted to yield important transition probabilities.⁵⁶ The short molecular axis phase arrangement (sum of the dipole moments along the *c* axis of Figure S4 in the Supporting Information) results in lowering the energy and gives rise to the band at longer wavelengths. The in-phase arrangement (sum of the dipole moments parallel to the *b* axis) raises the transition energy and corresponds to the band at shorter wavelengths. The broadening and rise of the baseline could be due to Mie scattering since all samples produce micrometer-sized bigger particles. Time-dependence absorption studies of **3** and **4** showed very similar absorption changes.

CH₃CN solutions of CDPA exhibit luminescence λ_{max} at 511 nm; again this becomes red-shifted on injection into acidic water (λ_{max} 585 nm). With increasing time, this luminescence λ_{max} gradually blue shifts to 551 nm, providing information on nano/microparticles formation. The excitation spectra mirror the absorption data as expected. There is a decrease in intensity of the signal at 430 nm until after 6 h, when new peaks appear at 366 and 500 nm (Figure S3 in the Supporting Information).

CDPA crystals grown from CH₃CN solution show different solid-state luminescence on grinding blue shifts the luminescence from λ_{max} 604 to 587 nm (Figure S5 in the Supporting Information). The formation of spherical amorphous particles (**1** and **2**) also leads to the blue shifting of luminescence λ_{max} from 604 to 551 nm. The diamond-shaped CDPA microcrystals of **3** and **4** shows two luminescence λ_{max} at 541 and 604 nm. Interestingly, **5**, which contains a higher proportion of multifaceted microcrystals, exhibits an intense peak at 587 nm and smaller peaks at 541 and 604 nm. The morphologies of organic nano/microparticles are known to alter the luminescence properties of organic materials.⁵⁷ The luminescence λ_{max} at 541 nm suggests the possibility of a fine amorphous powder along with the microcrystals. In fact the fluorescence lifetime monitored at 541 nm is very similar to that of the spherical amorphous particles (Table 2). FE-SEM studies also revealed the presence of fine amorphous powder in the solution (Figure S6 in the Supporting Information). The luminescence spectra of **1–6** are shown in Figure 9c. The spectra for **7** and **8** are very similar to the luminescence spectra of **6** (Figure 10).

The repeated appearance of luminescence λ_{max} at 604 nm of the diamond microcrystals of **3–6** indicates that the luminescence observed for the bulk crystals of CDPA is indeed a real peak and the blue shifting of luminescence λ_{max} by powdering

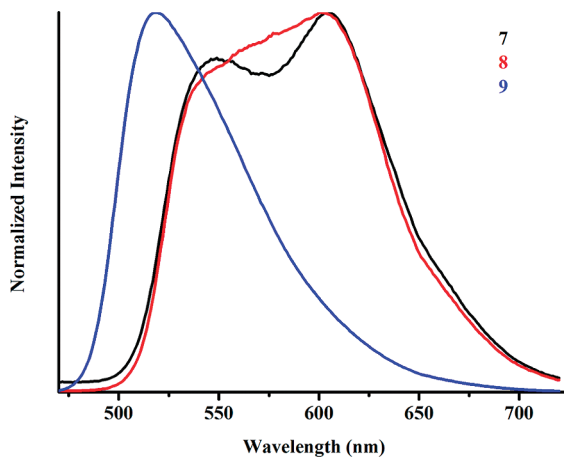


Figure 10. Luminescence spectra of **7–9** (refer to Table 1).

CDPA crystals might be due to the disruption of intermolecular interactions or change of morphology.

The size-dependent optical properties of organic nano/microstructures are generally understood on the basis of variations in intermolecular interactions as the particle size grows. The larger ratio of surface-to-bulk molecules at nanoscopic sizes makes the lattice relatively soft, such that as the particle size increases, the rigidity of the lattice improves and the intermolecular interactions strengthen.^{2,14,15} In smaller particles, only the strongest intermolecular interactions survive and other weak interactions evolve as the particle grows. As highlighted by Patra et al., the weak and varied nature of intermolecular interactions in molecular crystals should lead to a hierarchy of intermolecular forces that assert their influence in the structure formation as the nanocrystals grow.⁵⁸ Although weak, the varied intermolecular interactions are known to alter the energy levels of organic compounds.^{59,60}

To obtain further information on the nature, structure, and stability of the excited state, we measured the fluorescence lifetimes of CDPA in CH₃CN and CDPA nano/microstructures dispersed in HCl solution (Table 2). Decays were monitored at the corresponding emission maxima. Decay profiles of CDPA in CH₃CN solution and nano/microstructures are shown in Figure 11 and a systematic variation from solution-to-amorphous-to-microcrystals has been found. A systematic increase in the excited-state lifetimes was observed on going from solution, to amorphous, to microcrystals. Decays monitored in CH₃CN solution could be fitted monoexponentially, indicating a singlet excited state was exclusively formed. Nano/microstructured CDPA showed biexponential decay, suggesting the involvement of multiple excited states. Interestingly, the lifetime of the multifaceted microcrystals monitored at 587 nm were very close to the lifetime of powdered CDPA, adding further support to the idea that the blue shift of the luminescence could be due to

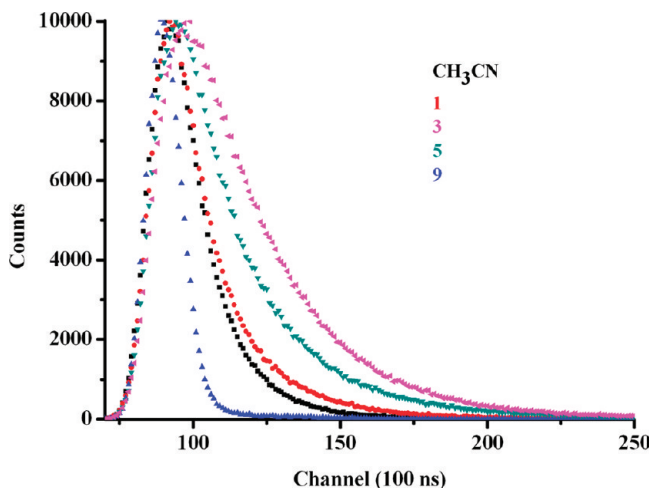


Figure 11. Fluorescence decay profiles (monitored at emission maxima and $\lambda_{\text{exc}} = 370 \text{ nm}$).

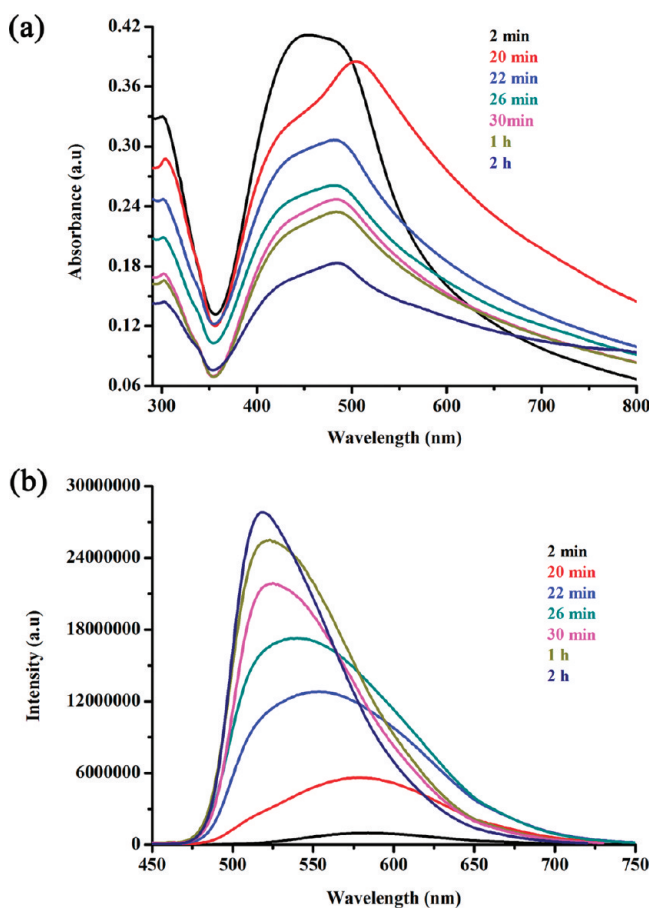


Figure 12. Time-dependent absorption (a) and luminescence (b) spectra of **9** (refer to Table 1).

the disruption of weak intermolecular interactions or change of morphology.

Time-dependent absorption and luminescence spectra of CDPA nanowires (**9**) are shown in Figure 12. The evolution of the nanowires was fast (2 h) compared to that of amorphous particles (24 h) and, once formed, the spectral profiles remain unchanged. Broad absorptions (440–500 nm) with λ_{max} at 450 nm were observed initially (within 2–5 min after injecting CDPA–CH₃CN into diluted HCl), but after 20 min, clear shoulders appeared at λ_{max} 429 and 505 nm that blue-shifted with time to 416 and 483 nm. As discussed earlier, the

appearance of two absorption bands can be understood based on exciton theory. The difference in the Davydov splitting might be due to the different intermolecular distance in the nanowires. The intensity of the absorption continuously decreased with time. The luminescence λ_{max} of CDPA in diluted HCl solution also blue-shifted (λ_{max} from 585 to 519 nm) in a 2 h time period. Nanowires formed in the presence of PAA exhibited a similar luminescence λ_{max} at 519 nm. The completely different luminescence λ_{max} for nanowires is expected due to the polymorphic structure.²⁰ The excitation spectra of the nanowires differ significantly from those of amorphous spheres or microcrystals and clearly matched the nanowire absorption spectra. Their fluorescent lifetimes were significantly shorter and the fluorescence decay profiles could be fitted monoexponentially, indicating a singlet excited state was exclusively formed (Figure 11, Table 2).

Conclusions

We have demonstrated that the solid-state luminescence properties of CDPA, a functional organic material, can be tuned by fabricating different nano/microstructures. Spherical amorphous, diamond, and multifaceted microcrystals of CDPA were obtained by controlling the fabrication conditions. The introduction of polymer additives to inhibit the crystal growth via adsorption on the surface of microcrystals led to the formation of 1D rods. Importantly, a polymorphic phase of CDPA, not observed by the usual crystallization approaches, was obtained as 1D nanowires. The polymorphic structure of nanowire CDPA was confirmed by powder X-ray diffraction and optical studies. The change of phase, morphology, and structure were accompanied by changes in the luminescence. The scope for tuning the optoelectronic properties of CDPA as a function of morphology, coupled with the formation of luminescent 1D nanowires, indicates that this organic chromophore might be a potential candidate in optical waveguide applications. In a wider context, nanofabrication might prove a versatile approach to obtaining new polymorphic structures of organic functional materials with tailored physical and optical properties.

Acknowledgment. This material is based on work supported by EU FP6 [MKT-D-CT-2004-014472] and Science Foundation Ireland [05PICA1819].

Supporting Information Available: CDPA crystal structure, confocal fluorescence and scanning electron microscopy images, FT-IR and luminescence spectra, and fluorescence lifetime decay profiles of CDPA–CH₃CN, CDPA crystals, CDPA powdered powders, **1**, **3**, **5**, **7**, and **9**. This material is available free of charge via the Internet at <http://pubs.acs.org>.

References and Notes

- (1) Kasai, H.; Nalwa, H. S.; Oikawa, H.; Okada, S.; Matsuda, H.; Minami, N.; Kakuta, A.; Ono, K.; Mukoh, A.; Nakanishi, H. A Novel Preparation Method of Organic Microcrystals. *Jpn. J. Appl. Phys.* **1992**, *31*, L1132–L1134.
- (2) Kasai, H.; Kamatani, H.; Okada, S.; Oikawa, H.; Matsuda, H.; Nakanishi, H. Size-Dependent Colors and Luminescences of Organic Microcrystals. *Jpn. J. Appl. Phys.* **1996**, *35*, L221–L223.
- (3) Yu, J.; Fan, F.-R. F.; Pan, S.; Lynch, V. M.; Omer, K. M.; Bard, A. J. Spontaneous Formation and Electrogenerated Chemiluminescence of Tris(bipyridine) Ru(II) Derivative Nanobelts. *J. Am. Chem. Soc.* **2008**, *130*, 7196–7197.
- (4) Takazawa, K.; Kitahama, Y.; Kimura, Y.; Kido, G. Optical Waveguide Self-Assembled from Organic Dye Molecules in Solution. *Nano Lett.* **2005**, *5*, 1293–1296.
- (5) Wang, J.; Zhao, Y.; Zhang, J.; Zhang, J.; Yang, B.; Wang, Y.; Zhang, D.; You, H.; Ma, D. Assembly of One-Dimensional Organic

- Luminescent Nanowires Based on Quinacridone Derivatives. *J. Phys. Chem. C* **2007**, *111*, 9177–9183.
- (6) O'Carroll, D.; Lieberwirth, I.; Redmond, G. Microcavity Effects and Optically Pumped Lasing in Single Conjugated Polymer Nanowires. *Nat. Nanotechnol.* **2007**, *2*, 180–184.
 - (7) Zhao, Y. S.; Peng, A.; Fu, H.; Ma, Y.; Yao, J. Nanowire Waveguides and Ultraviolet Lasers Based on Small Organic Molecules. *Adv. Mater.* **2008**, *20*, 1661–1665.
 - (8) Briseno, A. L.; Mannsfeld, S. C. B.; Lu, X.; Xiong, Y.; Jenekhe, S. A.; Bao, Z.; Xia, Y. Fabrication of Field-Effect Transistors from Hexathiapentacene Single-Crystal Nanowires. *Nano Lett.* **2007**, *7*, 668–675.
 - (9) Xiao, D.; Yang, W.; Yao, J.; Xi, L.; Yang, X.; Shuai, Z. Size-Dependent Exciton Chirality in (R)-(+)-1,1'-Bi-2-naphthol Dimethyl Ether Nanoparticles. *J. Am. Chem. Soc.* **2004**, *126*, 15439–15444.
 - (10) Fu, H.; Loo, B. H.; Xiao, D.; Xie, R.; Ji, X.; Yao, J.; Zhang, B.; Zhang, L. Multiple Emissions from 1,3-Diphenyl-5-pyrenyl-2-pyrazoline Nanoparticles: Evolution from Molecular to Nanoscale to Bulk Materials. *Angew. Chem., Int. Ed.* **2002**, *41*, 962–965.
 - (11) Kim, D. H.; Lee, D. Y.; Lee, H. S.; Lee, W. H.; Kim, Y. H.; Han, J. I.; Cho, K. High-Mobility Organic Transistors Based on Single-Crystalline Microribbons of Triisopropylsilylethynyl Pentacene via Solution-Phase Self-Assembly. *Adv. Mater.* **2007**, *19*, 678–682.
 - (12) Zhang, L.; Che, Y.; Moore, J. S. One-Dimensional Self-Assembly of Planar π -Conjugated Molecules: Adaptable Building Blocks for Organic Nanodevices. *Acc. Chem. Res.* **2008**, *41*, 1596–1608.
 - (13) Zhao, Y. S.; Fu, H.; Peng, A.; Ma, Y.; Xiao, D.; Yao, J. Low-Dimensional Nanomaterials Based on Small Organic Molecules: Preparation and Optoelectronic Properties. *Adv. Mater.* **2008**, *20*, 2859–2876.
 - (14) Briseno, A. L.; Mannsfeld, S. C. B.; Jenekhe, S. A.; Bao, Z.; Xia, Y. Introduction to Organic Nanowire Transistors. *Mater. Today* **2008**, *11*, 38–47.
 - (15) Oikawa, H.; Mitsui, T.; Onodera, T.; Kasai, H.; Nakanishi, H.; Sekiguchi, T. Crystal Size Dependence of Fluorescence Spectra from Perylene Nanocrystals Evaluated by Scanning Near-Field Optical Microspectroscopy. *Jpn. J. Appl. Phys.* **2003**, *42*, L111–L113.
 - (16) Volkov, V. V.; Asahi, T.; Masuhara, H.; Masuhara, A.; Kasai, H.; Oikawa, H.; Nakanishi, H. Size-Dependent Optical Properties of Polydiacetylene Nanocrystal. *J. Phys. Chem. B* **2004**, *108*, 7674–7680.
 - (17) Li, S.; He, L.; Xiong, F.; Li, Y.; Yang, G. Enhanced Fluorescent Emission of Organic Nanoparticles of an Intramolecular Proton Transfer Compound and Spontaneous Formation of One-Dimensional Nanostructures. *J. Phys. Chem. B* **2004**, *108*, 10887–10892.
 - (18) Han, M.; Hara, M. Intense Fluorescence from Light-Driven Self-Assembled Aggregates of Nonionic Azobenzene Derivative. *J. Am. Chem. Soc.* **2005**, *127*, 10951–10955.
 - (19) Zhao, Y. S.; Wu, J.; Huang, J. Vertical Organic Nanowire Arrays: Controlled Synthesis and Chemical Sensors. *J. Am. Chem. Soc.* **2009**, *131*, 3158–3159.
 - (20) Che, Y.; Zang, L. Enhanced Fluorescence Sensing of Amine Vapor Based on Ultrathin Nanofibers. *Chem. Commun.* **2009**, 5106–5108.
 - (21) Wang, Y.; Fu, H.; Peng, A.; Zhao, Y.; Ma, J.; Ma, Y.; Yao, J. Distinct Nanostructures from Isomeric Molecules of Bis(Iminopyrrole) Benzenes: Effects of Molecular Structures on Nanostructural Morphologies. *Chem. Commun.* **2007**, 1623–1625.
 - (22) Schenning, A. P. H. J.; Meijer, E. W. Supramolecular Electronics; Nanowires from Self-Assembled Π -Conjugated Systems. *Chem. Commun.* **2005**, 3245–3258.
 - (23) Löwik, D.; Shklyarevskiy, I. O.; Ruizendaal, L.; Christianen, P. C. M.; Maan, J. C.; van Hest, J. C. M. A Highly Ordered Material from Magnetically Aligned Peptide Amphiphile Nanofiber Assemblies. *Adv. Mater.* **2007**, *19*, 1191–1195.
 - (24) Ajayaghosh, A.; Praveen, V. K. π -Organogels of Self-Assembled *p*-Phenylenevinylenes: Soft Materials with Distinct Size, Shape, and Functions. *Acc. Chem. Res.* **2007**, *40*, 644–656.
 - (25) Balakrishnan, K.; Datar, A.; Oitker, R.; Chen, H.; Zuo, J.; Zhang, L. Nanobelts Self-Assembly from an Organic n-Type Semiconductor: Propoxyethyl-PTCDI. *J. Am. Chem. Soc.* **2005**, *127*, 10496–10497.
 - (26) Zhang, X.; Zhang, X.; Shi, W.; Meng, X.; Lee, C.; Lee, S. Single-Crystal Organic Microtubes with a Rectangular Cross Section. *Angew. Chem., Int. Ed.* **2007**, *46*, 1525–1528.
 - (27) Zhang, X.; Zhang, X.; Zou, K.; Lee, C. S.; Lee, S. T. Single-Crystal Microribbons, Nanotubes, and Nanowires from Intramolecular Charge-Transfer Organic Molecules. *J. Am. Chem. Soc.* **2007**, *129*, 3527–3532.
 - (28) Jordan, B. J.; Ofir, Y.; Patra, D.; Caldwell, S. T.; Kennedy, A.; Joubanian, S.; Rabani, G.; Cooke, G.; Rotello, V. M. Controlled Self-Assembly of Organic Nanowires and Platelets Using Dipolar and Hydrogen-Bonding Interactions. *Small* **2008**, *4*, 2074–2078.
 - (29) Katagi, H.; Kasai, H.; Okada, S.; Oikawa, H.; Matsuda, H.; Nakanishi, H. Preparation and Characterization of Poly-Diacetylene Microcristals. *J. Macromol. Sci., Pure Appl. Chem.* **1997**, *34*, 2013–2024.
 - (30) Nakanishi, H.; Katagi, H. Microcrystals of Polydiacetylene Derivatives and Their Linear and Nonlinear Optical Properties. *Supramol. Sci.* **1998**, *5*, 289–295.
 - (31) Nalwa, H. S.; Kasai, H.; Okada, S.; Oikawa, H.; Matsuda, H.; Kakuta, H.; Mukoh, A.; Nakanishi, H. Fabrication of Organic Nanocrystals for Electronics and Photonics. *Adv. Mater.* **1993**, *5*, 758–760.
 - (32) Onodera, T.; Oshikiri, T.; Katagi, H.; Kasai, H.; Okada, S.; Oikawa, H.; Terauchi, M.; Tanaka, M.; Nakanishi, H. Nanowire Crystals of π -Conjugated Organic Materials. *J. Cryst. Growth* **2001**, *229*, 586–590.
 - (33) Davis, R.; Rath, N. P.; Das, S. Thermally Reversible Fluorescent Polymorphs of Alkoxy-Cyano-Substituted Diphenylbutadienes: Role of Crystal Packing in Solid State Fluorescence. *Chem. Commun.* **2004**, 74–75.
 - (34) Mutai, T.; Tomoda, H.; Ohkawa, T.; Yabe, Y.; Araki, K. Switching of Polymorph-Dependent ESIPT Luminescence of an Imidazo[1,2-*a*]pyridine Derivative. *Angew. Chem., Int. Ed.* **2008**, *47*, 9522–9524.
 - (35) Mutai, T.; Satou, H.; Araki, K. Reproducible On-Off Switching of Solid-State Luminescence by Controlling Molecular Packing through Heat-Mode Interconversion. *Nat. Mater.* **2005**, *4*, 685–687.
 - (36) Bernstein, J. *Polymorphism in Molecular Crystals*; Oxford: New York, 2002.
 - (37) Tsekova, D. S.; Escuder, B.; Miravet, J. F. Solid-State Polymorphic Transition and Solvent-Free Self-Assembly in the Growth of Organic Crystalline Microfibers. *Cryst. Growth Des.* **2008**, *1*, 11–13.
 - (38) Ha, J.-M.; Hamilton, B. D.; Hillmyer, M. A.; Ward, M. D. Phase Behavior and Polymorphism of Organic Crystals Confined within Nanoscale Chambers. *Cryst. Growth Des.* **2009**, *9*, 4766–4777.
 - (39) Yu, L.; Cebe, P. Crystal Polymorphism in Electrospun Composite Nanofibers of Poly(Vinylidene Fluoride) with Nanoclay. *Polymer* **2009**, *50*, 2133–2141.
 - (40) van der Laan, S.; Feringa, B. L.; Kellogg, R. M.; van Esch, J. Remarkable Polymorphism in Gels of New Azobenzene Bis-Urea Gelators. *Langmuir* **2002**, *18*, 7136–7140.
 - (41) Shih, P.-I.; Chien, C.-H.; Wu, F.-I.; Shu, C.-F. A Novel Fluorene-Triphenylamine Hybrid That is a Highly Efficient Host Material for Blue-, Green-, and Red-Light-Emitting Electrophosphorescent Devices. *Adv. Funct. Mater.* **2007**, *17*, 3514–3520.
 - (42) Tian, Y.-P.; Li, L.; Zhang, J.-Z.; Yang, J.-X.; Zhou, H.-P.; Yu, J.-Y.; Sun, P.-P.; Tao, L.-M.; Guo, Y.-H.; Wang, C.-K.; Xing, H.; Hung, W.-H.; Tao, X.-T.; Jiang, M.-H. Investigations and Facile Synthesis of a Series of Novel Multi-Functional Two-Photon Absorption Materials. *J. Mater. Chem.* **2007**, *17*, 3646–3654.
 - (43) Kitamura, T.; Ikeda, M.; Shigaki, K.; Inoue, T.; Anderson, N. A.; Ai, X.; Lian, T.; Yanagida, S. Phenyl-Conjugated Oligoene Sensitizers for TiO₂ Solar Cells. *Chem. Mater.* **2004**, *16*, 1806–1812.
 - (44) Ning, Z.; Chen, Z.; Zhang, Q.; Yan, Y.; Qian, S.; Cao, Y.; Tian, H. Aggregation-Induced Emission (AIE)-Active Starburst Triarylamine Fluorophores as Potential Non-Doped Red Emitters for Organic Light-emitting Diodes and Cl₂ Gas Chemodosimeter. *Adv. Funct. Mater.* **2007**, *17*, 3799–3807.
 - (45) Patra, A.; Anthony, S. P.; Radhakrishnan, T. P. Tris(4-cyanophenyl)amine: Simple Synthesis via Self-assembly; Strong Fluorescence in Solution, Nano/Microcrystals and Solid. *Adv. Funct. Mater.* **2007**, *17*, 2077–2084.
 - (46) Anthony, S. P.; Varughese, S.; Draper, S. M. Switching and Tuning Organic Solid-State Luminescence via a Supramolecular Approach. *Chem. Commun.* **2009**, 7500–7502.
 - (47) Hagberg, D. P.; Marinado, T.; Kalsson, K. M.; Nonomura, K.; Qin, P.; Boschloo, G.; Brinck, T.; Hadfeldt, A.; Sun, L. Tuning the HOMO and LUMO Energy Levels of Organic Chromophores for Dye Sensitized Solar Cells. *J. Org. Chem.* **2007**, *72*, 9550–9556.
 - (48) Bertorelle, F.; Rodrigues, F.; Fery-Forgues, S. Dendrimer-Tuned Formation of Fluorescent Organic Microcrystals. Influence of Dye Hydrophobicity and Dendrimer Charge. *Langmuir* **2006**, *22*, 8523–8531.
 - (49) Birla, L.; Bertorelle, F.; Rodrigues, F.; Badré, S.; Pansu, R.; Fery-Forgues, S. Effects of DNA on the Growth and Optical Properties of Luminescent Organic Microcrystals. *Langmuir* **2006**, *22*, 6256–6265.
 - (50) Abyan, M.; de Caro, D.; Fery-Forgues, S. Suspensions of Organic Microcrystals Produced in the Presence of Polymers: Diversity of UV/Vis Absorption and Fluorescence Properties According to the Preparation Conditions. *Langmuir* **2009**, *25*, 1651–1658.
 - (51) Lei, Y.; Liao, Q.; Fu, H.; Yao, J. Phase- and Shape-Controlled Synthesis of Single Crystalline Perylene Nanosheets and Its Optical Properties. *J. Phys. Chem. C* **2009**, *113*, 10038–10043.
 - (52) Silverstein, R. M.; Webster, F. X.; Kiemle, D. J. *Spectrometric Identification of Organic Compounds*, 7th ed.; Wiley: New York, 2005; Chapter 2, pp 72–126.
 - (53) Kasha, M.; Rawls, H. R.; El-Bayoumi, M. A. The Exciton Model in Molecular Spectroscopy. *Pure Appl. Chem.* **1965**, *11*, 371–392.
 - (54) Davidov, A. S. *Theory of Molecular Excitons*; McGraw-Hill: New York, 1962.

- (55) Kirstein, S.; Möhwald, H. Structure and Optical Properties of a Monolayer Single Crystal of a Cyanine Dye. *Chem. Phys. Lett.* **1992**, *189*, 408–413.
- (56) Czikkely, V.; Försterling, H. D.; Kuhn, H. Light Absorption and Structure of Aggregates of Dye Molecules. *Chem. Phys. Lett.* **1970**, *6*, 11–14.
- (57) Zhang, X.; Dong, C.; Zapien, J. A.; Ismathullah Khan, S.; Kang, Z.; Jie, J.; Zhang, J. C.; Lee, C. S.; Lee, S. T. Polyhedral Organic Microcrystals: From Cubes to Rhombic Dodecahedra. *Angew. Chem., Int. Ed.* **2009**, *48*, 9121–9123.
- (58) Patra, A.; Hebalkar, N.; Sreedhar, B.; Sarkar, M.; Samanta, A.; Radhakrishnan, T. P. Tuning the Size and Optical Properties in Molecular Nano/Microcrystals: Manifestation of Hierarchical Interactions. *Small* **2006**, *2*, 650–659.
- (59) Birks, J. B. *Photophysics of Aromatic Molecules*; Wiley: London, 1970.
- (60) Silinsh, E. A. *Organic Molecular Crystals*; Springer-Verlag: Berlin, 1980.

JP100594W